PROJECT PROGRESS REPORT
For Period: 2/01/2012 - 07/31/2013
(Second semiannual report for FY 2)

Award Number:	NA11NES4400002
Award Period:	08/01/2011 - 07/31/2014
Project Title:	Development of new 3-hourly, global, long-term, multisatellite-based TOA-to-surface radiative flux profile data product with high horizontal resolution and homogeneous quality
Recipient Name:	The Trustees of Columbia University in the City of New York
Project PI:	Yuanchong Zhang
Report Type:	Semiannual Project Progress Report
Reported by:	Yuanchong Zhang

Planned Tasks for the Year 2 in the proposal:

- 1. Creation of new production codes
- 2. New product processing
- 3. Reengineering all the codes
- 4. Evaluation of new codes and products

1. Creation of new production codes

(1) Status of RadE-1

The new ISCCP H-series product is about to begin as we just tested two versions of ISCCP-FD-like ISCCP H-series product with ISCCP-FD production code; the version 0 of RadE-1 ('RadE-1_0') will be made available for ingesting and testing the new H-series product once it comes out while waiting for the fulfillment of the all improvement parts of radiation code development (see below) that will eventually be developed for revising RadE_1 to the new ISCCP-FH's radiation subroutine package (or base code), RadH, of ISCCP-FH's production code.

(2) Model improvements

Although the planned LW improvements have been completed and validated (see previous reports), the GISS radiation group is now making further improvements on the current RadE that will also applied to new RadH.

While the major work on improving SW flux calculation has been completed, there are a few possible improvements are to be done after the said new, additional LW improvements are finished.

The main efforts then have been focused on new vertical cloud layer configuration, which may be implemented by two schemes for setting (1) Cloud Vertical Structure (CVS) that determines the number of overlapped cloud layers and how they are related (separated or connected) and (2) cloud layer thickness that determines physical positions of each of all the cloud layers of a CVS type. These two schemes are necessary because ISCCP cloud climatology only supplies upmost cloud pressure (PC) along with total column cloud optical thickness (Tau) of a specific cloud type that are not sufficient for configure the physical positions of all possible, vertically distributed cloud layers. As the problem is not physically well posed and may not be fully resolved in any foreseen future by either observation or theory at the spatiotemporal resolution and coverage of ISCCP, we have to rely on physically reasonable hypothesis as we have tried for ISCCP-FD production, in which, our primary schemes have been proved reasonably good (Rossow and Zhang 2010). As we have better CloudSat and CALIPSO observations for cloud vertical structure, we intend to have a better cloud layer configuration implementation as one of the major improvements for ISCCP-FH production.

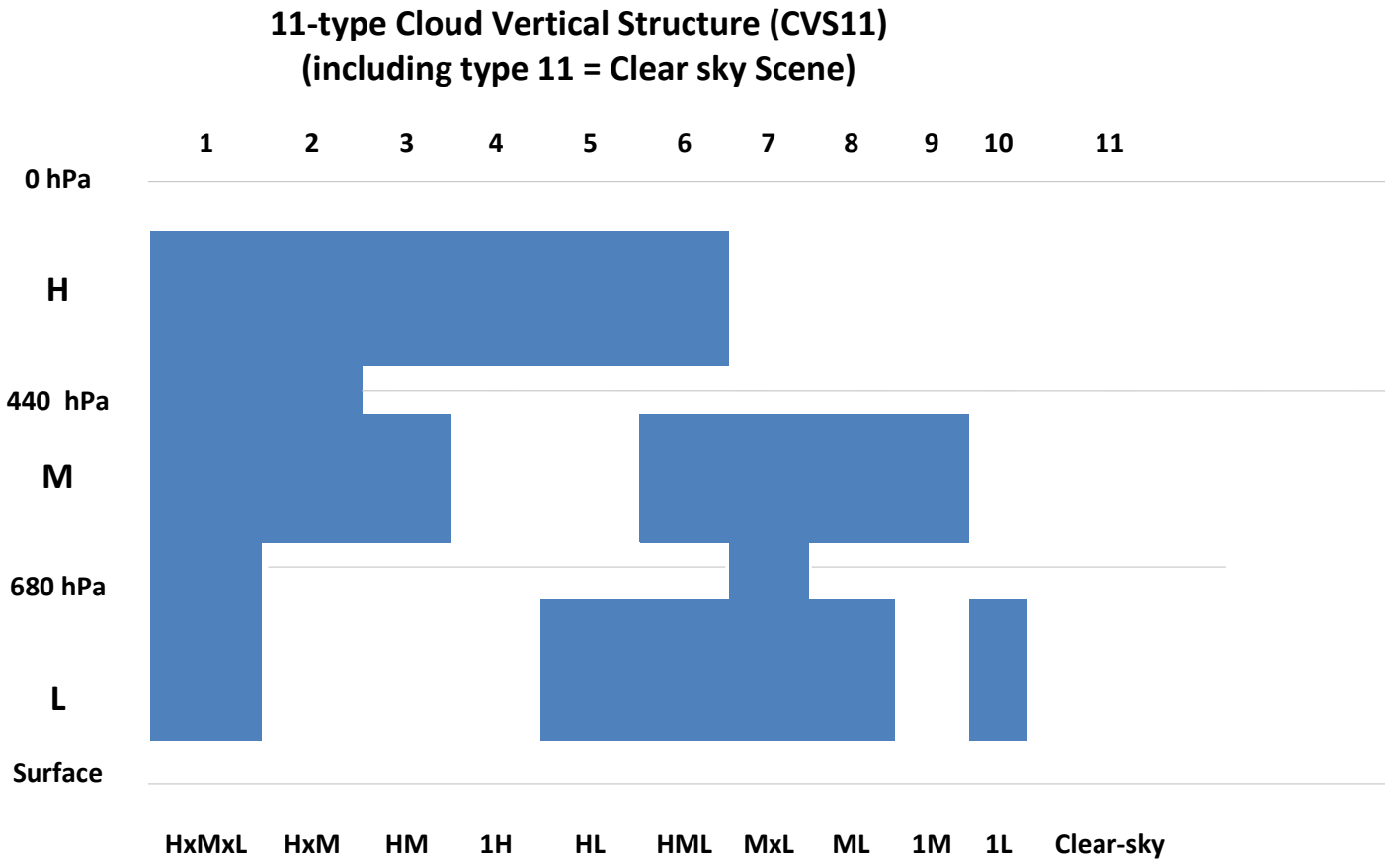

Fig. 1. Ten CVS types with an additional clear-sky scene (type 11): H/M/L=high/Middle/Low clouds as indicated; cloud layers for different CVS types are schematically shown, either vertically separated (e.g., HML, type 6) or connected (e.g., HxMxL, type 1).

The (new) eleven CVS types (ten for clouds) are illustrated in Fig. 1, which has two more CVS types, HxM and MxL, in addition to our old CVS model's eight CVS types for ISCCP-FD production. All ISCCP clouds are categorized to high, middle and low clouds with their PC ranging from 0 to 440 hPa, 440 to 680 hPa, and 680 hPa to surface, respectively, as shown as H, M and L in Fig. 1. Each CVS type is statistically significant and has its distinctive vertical structure based on its cloud layer numbers and how the layers are overlapped .

In exploring a new CVS scheme, we have processed 5-year CloudSat and CALIPSO (C&C) 2B-TAU and 2B-GEOPROF-LIDAR datasets from Cloudsat Data Processing Center (http://www.cloudsat.cira.colostate.edu/), and exactly spatiotemporally matched them, i.e., each CVS type is actually related to total column cloud optical thickness (Tau) and PC based on the C&C observations. In addition, we have also spatiotemporally matched them with ISCCP-DX based CVS data for their overlapped three years (July 2006 to December 2009) as exemplified in Fig. 3. The relationship is processed for each month over the 5-yr (or 3-yr) period over global and seven latitudinal zones (South Polar, Southern Mid-latitudes, Southern sub-tropic, Tropic, Northern sub-tropic, Northern Mid-latitudes and North Polar), as contrasted to the one universal CVS model used in ISCCP-FD. For the ten CVS types (excluding clear-sky, type 11, Fig. 1), we have calculated their Relative Frequency Occurrence (RFO) and associate all RFOs to Tau (X) and PC (Y) to make their quasi-functional relationship and arrange their values in descending order, where Tau is divided into six ranges in consistency with the (old and new) ISCCP's Tau dividing for cloud types (and weather states), and PC for five ranges covering high and middle cloud PC altitudes (we don't need set CVS type for low cloud as it is always for one low cloud layer in cloud configuration) as contrast to old CVS model's coarser two PC ranges only for high and middle clouds, respectively. Also calculated is the ratio to the first largest RFO for all the other RFO (from the second-largest RFO to whichever available CVS type's RFO). In examining the 3-yr CVS climatology, virtually all the CVS types show that the ratio (to the first largest RFO) of the third largest RFO has converged to ≤ 50% and about 1/2 grids' ratio values have become ~20% or lower, which indicates that we may use the first two largest-RFO CVS types to reasonably well represent actual CVS types for flux calculation without losing statistical significance and vertical structure diversities.

As an example and for simplicity, we show the CVS types with the first and second largest RFO, respectively, for global (i.e., all together of seven latitudinal zones) ocean and land for July over the 3-yr (2006—2008) period in Fig. 2a and 2b and old CVS model for ISCCP-DX over the same period in Fig. 3.

Fig. 2a shows that, for high clouds, both ocean and land show that 1H (CVS type 1) is associated with lowest Tau values (at higher altitude), which was similarly assumed in ISCCP-FD based on much sparse, 20-yr rawinsonde climatology (primary over Northern Hemispheric land areas, Rossow et al. 2005; Rossow and Zhang, 2010), but somewhat different as the latter has coarser vertical resolution as shown in Fig. 3; HxMxL (type 6) also appears in high-Tau range as in old CVS model (Fig. 3) but extended to lower Tau range where old model is HML (Tau = [9.38,22.63]) and HM (Tau = [3.55, 9.38] with a few exceptions that are for HxM at lower PS of [310, 440] and low Tau., but HxM is a new CVS type separated from old 1H. HML begins to appears in the fifth largest RFO for ocean and sixth largest for land for the new C&C-

based histograms and HM appears from the second largest RFO and onwards (not shown). Fig. 2a shows that the first-largest high-cloud CVS is physically rational as the old CVS model but new CVS model may be more accurate (with some uncertainties).

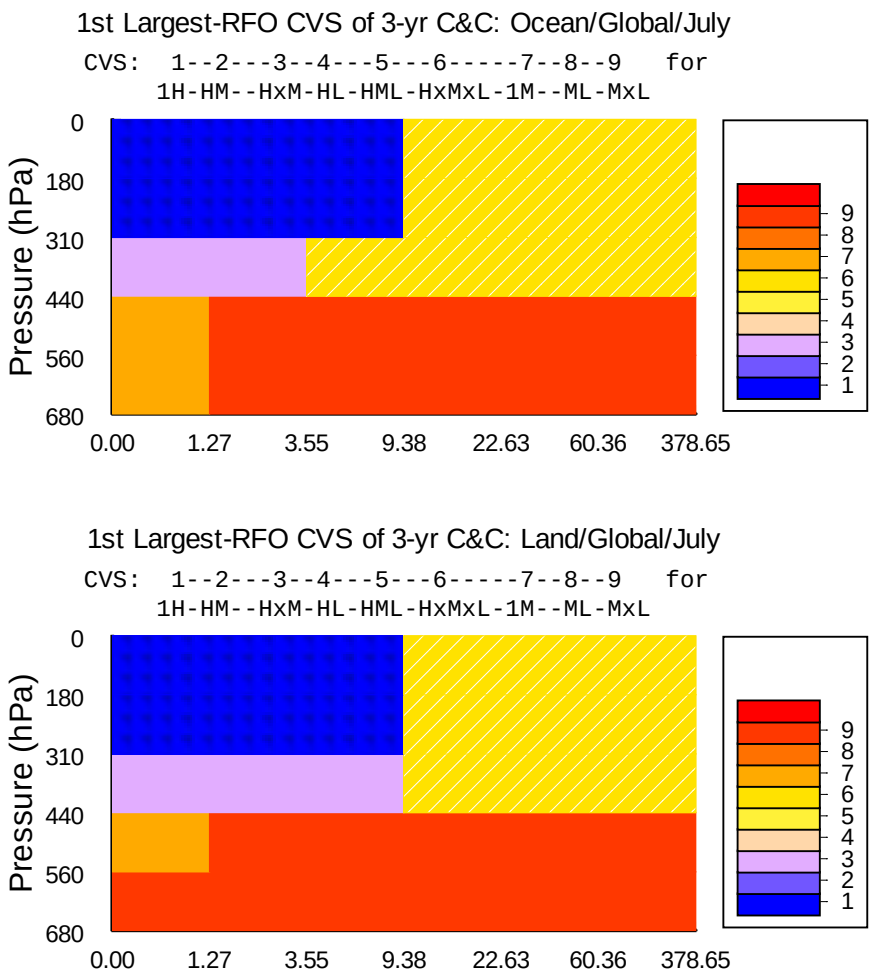

Fig. 2a. The CVS types with the first largest Relative Frequency Occurrence (RFO) for high and middle clouds for July of 2006-2008 period for global ocean (upper) and land (lower), respectively, as function of Tau and PC. The nine high and middle cloud CVS types are illustrated at the headlines.

For middle-cloud CVS, the new CVS histogram is the same as the old one except PC of [560, 680 hPa] for Tau of [0.00, 1.27] for land and the new type MxL (type 9) replaces old ML (type 8). Note that old CVS (Fig. 3) ascribed Tau of [1.27, 9.39] to HL, moved out from middle clouds;

it is expected to have lower RFO values but it cannot be shown for this processing because this HL is implemented by resetting PC to be high clouds' in flux calculation that is not conducted here.

Fig. 2b shows the second largest RFO's CVS types. They are essentially 2- or 3-layer CVS with one exceptional grids of 1H for Tau = [9.38, 22.63] and PC = [0, 180] for land but its RFO ratio (to the first largest) is ~60%. The HxMxL (type 6) appears in lower Tau range (Tau ≤ 0.355) especially for land but their RFO ratio is lower (≤ 50%) for Tau ≤ 3.55 so it is not necessarily unrealistic.

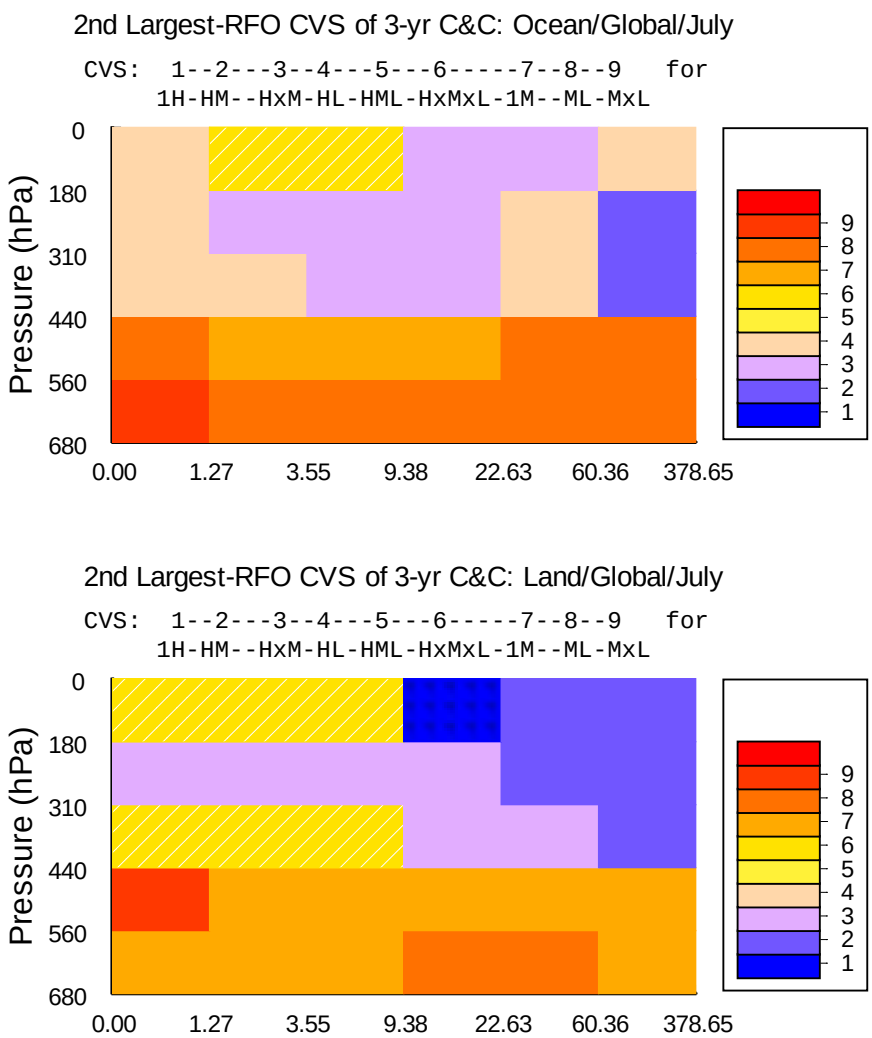

Fig. 2b. Same as Fig. 1a but for the second largest RFO's CVS types.

Overall, Fig. 2 shows that the observation-based new CVS histogram seems physically plausible. We may combine the first and second largest RFO's CVS types to represent cloud amount of each of the new H-series ISCCP's 18 cloud types (defined by their Tau, PC, and phase with additional three liquid high cloud types from D-series) with their sub-divided cloud amounts proportional to the (normalized) RFO values. By this way, the new CVS model may better represent the true cloud fields and their vertical structure.

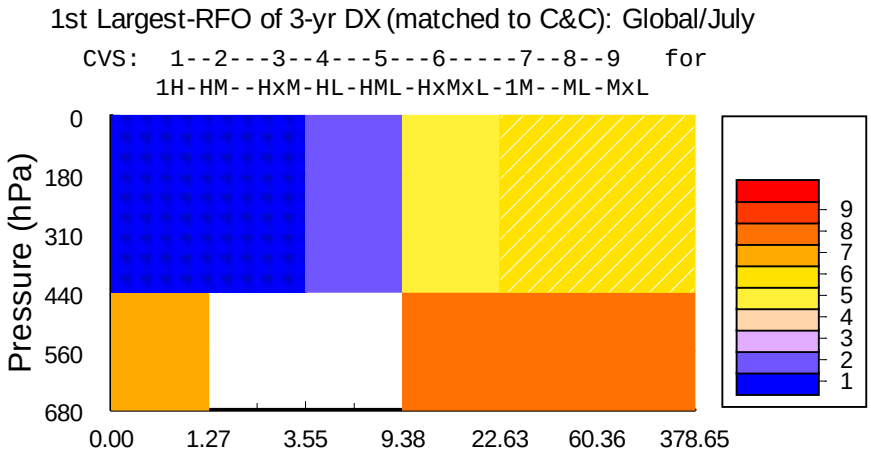

Fig. 3. CVS model for previous ISCCP-FD based on 3-yr ISCCP-DX spatiotemporally matched to C&C (CVS + Tau) profile (PC difference ≤ 50 mb). Note, there is only one deterministic CVS model for all global ocean and land and the middle-cloud blank areas is set to HL that does not appear in this processing.

With new CVS model, we also need better-based cloud layer thickness climatology. The cloud thickness for ISCCP-FD is a function of 10°-latitudinal zones (ocean and land are separated) based on the 20-yr rawinsonde data. We now use 5-yr C&C that has much large sampling size. The new cloud thickness has two additional independent variables, 40°-longitudinal zone and three Tau ranges. Fig. 4 shows an example for comparing cloud layer thickness climatology between C&C and old rawinsonde-based, where C&C has been averaged over longitudinal zones and Tau ranges for the comparison. The figure shows that, old thickness generally exaggerates at high altitudes (lower PC) and it is reversed over middle cloud PC ranges. The introduction of Tau variable makes cloud layer thicker for higher Tau values and may automatically extends some 1-layer cloud to two connected cloud layers (i.e., crossing boundary between high, middle

and low clouds, e.g., 1H to actual HxM and 1M to actual MxL), which may compensates some shortfalls of the CVS histogram over high-tau ranges.

2. New product processing

(1) Make all input datasets available

The H-series ISCCP product will become available within a month or two when we can start working on the availability of all the input dataseets.

(2) Create new ingestion codes

Recently we tested two versions of ISCCP-FD-like ISCCP H-series product with ISCCP-FD production code. As the RadE-1_0 base code works for ingesting D-series-like H-series ISCCP, the real H-series ISCCP datasets (after necessary readjustment and changes) will be ingested to RadE-1 code that will gradually and progressively be built to the final production code with improved base radiation code and ancillary datasets.

3. Reengineering all the codes

Since the RadE-1_0 (current new code) has been primarily reengineered, it is ready to take in new input datasets and new code changes with necessary further reenginnering.

4. Evaluating new codes and products

We keep doing checking and validating work whenever the code is revised at every stage to make sure each revision is correct.

5. Short Summary

In short, over the second half year of the second fiscal year, we have mainly focused on vertical cloud layer configuration consisting of CVS mode and layer thickness climatology that is crucial for the new ISCCP-FH production. The project has generally been progressed as allowed by the reality that makes our work a little behind of the originally planned schedule but we still expect that all tasks be accomplished by the planned time period in the third year.

References

Rossow, W.B., Y-C. Zhang and J-H. Wang (2005), A statistical model of cloud vertical structure based on reconciling cloud layer amounts inferred from satellites and radiosonde humidity profiles. J. Climate, 18, 3587-3605.

Rossow, W.B and Y. Zhang (2010) Evaluation of a Statistical Model of Cloud Vertical Structure Using Combined CloudSat and CALIPSO Cloud Layer Profiles, *J. Climate*, 23, 6641-6653.

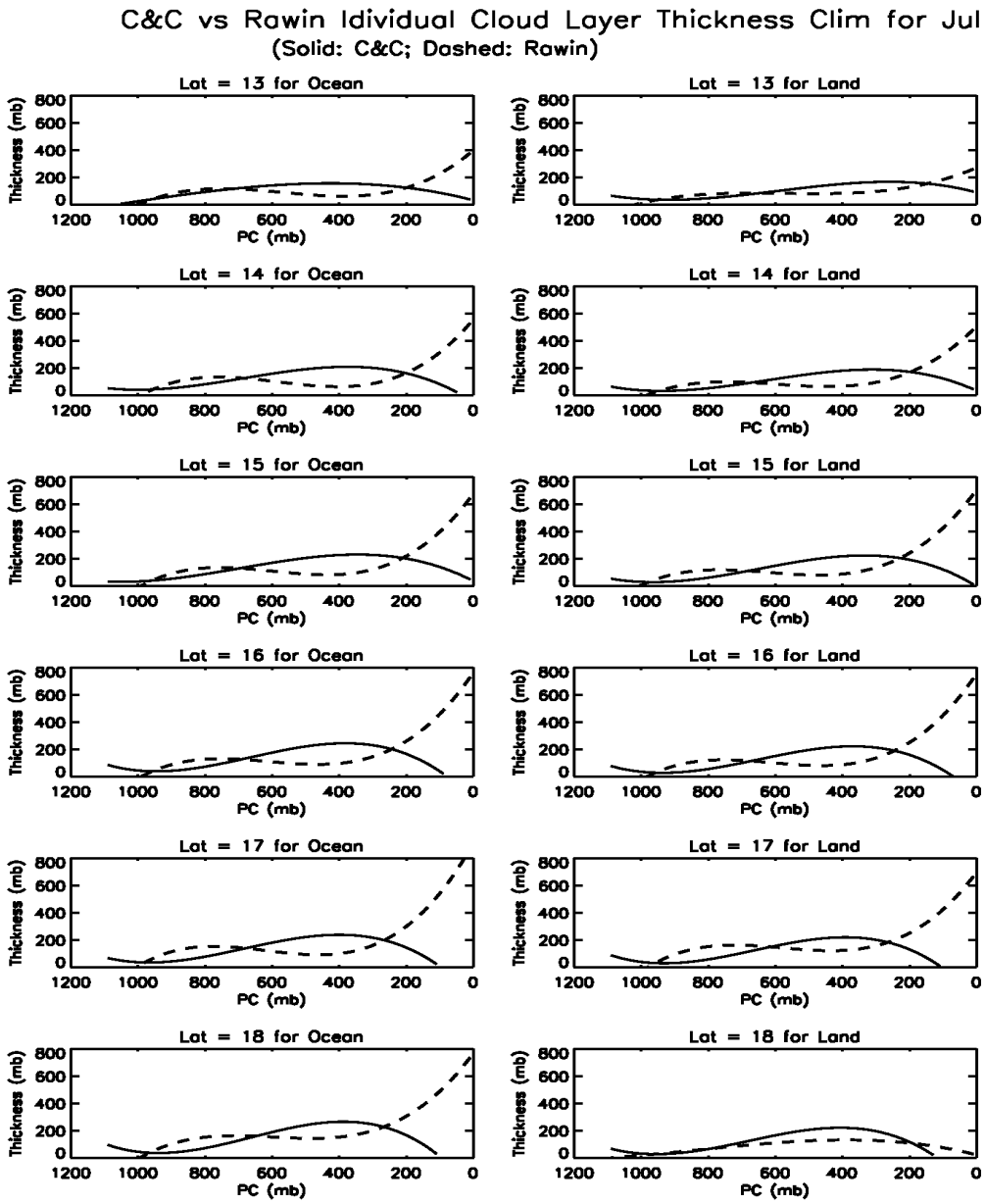

Fig. 4. Comparison of cloud layer thickness climatology between new from C&C (solid line) and old Rawinsonde("Rawin", dashed) for 10° latitudinal zones 13 (30° N to 40° N) to 18 (80° N to 90° N) for ocean and land, respectively, for July; X=PC in mb and Y=cloud thickness (mb). The new climatology has beed averaged over longitudinal zones and Tau for this comparison as Rawin is independent of the two variables.